Orbital Molecules in the New Spinel GaV2O4

Orbital molecules in the new spinel GaV_2O_4

Alexander J. Browne,[†] Calum Lithgow,[†] Simon. A. J. Kimber,[‡] and J. Paul Attfield*,[†]

[†]Centre for Science at Extreme Conditions and School of Chemistry, University of Edinburgh, West Mains Road, Edinburgh EH9 3FD, United Kingdom

[‡]Diffraction Group, Neutron Sciences Division, Oak Ridge National Laboratory, Oak Ridge, TN 37831, U.S.A.

ABSTRACT: The structures and properties of vanadium oxides are often related to the formation of molecule-like clusters of vanadium cations through direct V-V bonding. GaV_2O_4, a new vanadium spinel, has been synthesized. Powder diffraction and X-ray total scattering studies, complemented by magnetization and resistivity measurements, reveal that the low temperature phase of this material is structurally distorted and features ordered pairs of three- and four-atom vanadium clusters. These clusters persist into a disordered cubic phase above the charge ordering transition at T_{CO} = 415 K. Furthermore, quasi-elastic neutron scattering indicates that the disordered clusters remain well defined and static to 1100 K.

INTRODUCTION

The notable electronic properties of vanadium oxides have led to these materials finding numerous applications. Several systems, such as layered $Li_{1+x}V_{1-x}O_2$[1] and Na_xVO_2[2] phases and nanostructured V_2O_5,[3] are being investigated as battery electrode materials. Nanospheres of the spinel ZnV_2O_4 have promising supercapacitance and hydrogen storage properties;[4] BIMEVOX phases derived from γ-$Bi_4V_2O_{11}$ are a prominent family of oxide ion conductors;[5] and many vanadium oxides are used as catalysts.[6]

In some vanadium oxides, functionality is the result of an electronic ordering transition. A prominent example is VO_2, which undergoes an ultrafast metal-insulator transition at 340 K.[7] There is considerable interest in developing technology that exploits the dramatic change in properties associated with this transition, ranging from electronic switches to chemical sensors and thermochromic window coatings.[8,9]

At the metal-insulator transition, VO_2 undergoes changes to both its electronic and crystallographic structure. In the high temperature metallic phase there is a single V-V nearest-neighbor distance (2.87 Å), found along chains of edge-sharing VO_6 octahedra, but this splits into alternatingly short (2.65 Å) and long (3.12 Å) separations in the low temperature insulating regime.[10] This is an example of an orbital molecule state – the short V-V separations in insulating VO_2 define spin-singlet $(V^{4+})_2$ dimers. Orbital molecules are clusters of transition metal cations formed when orbital ordering localizes electrons into directly-interacting *d* orbitals,[11] and are found in the ground states of many vanadium oxides. Mixed-valence oxides such as V_4O_7, which are structurally related to VO_2, also exhibit metal-insulator transitions accompanied by V-V dimerization.[12] Triangular $(V^{3+})_3$ spin-singlet trimers form in $LiVO_2$ and $Li_{1+x}V_{1-x}O_2$ ($x \leq 0.1$),[13] and $BaV_{10}O_{15}$.[14] $NaVO_2$ undergoes orbital ordering without forming orbital molecules,[15] but interestingly the ground states of different polymorphs of $Na_{0.5}VO_2$, corresponding to different arrangements of the Na-site vacancies, exhibit different vanadium clusterings, and both dimer and trimer ground states have been found.[16] In all of these materials the formation of orbital molecules coincides with dramatic changes to their electronic structure, and hence to their electrical and magnetic properties.

Understanding the microscopic mechanism of orbital molecule formation is desirable for developing this behavior into functionality. Typically, V-V bonds emerge when a uniform structure distorts below an electronic transition temperature. In both VO_2 and $LiVO_2$, the distortion is driven by orbital polarizations that result in significant *d*-*d* σ-bonding interactions.[17,18] This is similar to the orbitally induced Peierls transition used to describe the formation of orbital dimer states in the spinels $CuIr_2S_4$ and $MgTi_2O_4$.[19]

However, we have recently found a very different type of orbital molecule behavior in the spinel AlV_2O_4.[20] Investigation of the local structure of this material through analysis of the pair distribution function (PDF) revealed ordered $(V^{3+})_3$ trimers and $(V^{2+})_4$ tetramers – the largest known orbital molecules – in the distorted $R\bar{3}m$ ground state, and not V_7^{17+} heptamers as previously proposed.[21] This ground state is the result of long-range orbital- and charge-ordering, corresponding to the electronic description $Al_4[V_4^{8+}V_3^{9+}V^{3+}]O_{16}$. Above the transition temperature T_{CO} = 700 K this long-range order is lost and the material has a

cubic $Fd\bar{3}m$ average structure with uniform V-V nearest-neighbor distances. However, short-range order is retained and the trimers and tetramers persist in a structurally disordered phase to at least 1100 K ($1.6T_{CO}$). This is consistent with magnetization and resistivity measurements, which show very little change across the transition temperature.[22] The stability of V-V bonding well above the long-range ordering temperature indicates a fundamentally different mechanism of orbital molecule formation in AlV_2O_4 than is found in other vanadium oxides – in the high temperature phase of VO_2, the dimers do not persist on either the long-range or local scale.[23]

Here we report the synthesis and characterization of GaV_2O_4, a new vanadium oxide spinel. It exhibits the complex orbital molecule behavior found in isoelectronic AlV_2O_4, but with a lower T_{CO} of 415 K, hence we demonstrate the persistence of disordered orbital molecules to the relatively higher temperature of $2.7T_{CO}$. Furthermore, we have used quasi-elastic neutron scattering (QENS) to investigate whether the orbital molecules have static or dynamic disorder at high temperatures.

EXPERIMENTAL SECTION

Synthesis. Polycrystalline GaV_2O_4 was synthesized by a high temperature solid state reaction. Powdered Ga_2O_3 (Sigma Aldrich, 99.99%), V (Alfa Aesar, 99.5%) and V_2O_5 (Alfa Aesar, 99.6%) in the stoichiometric ratio were ground together, pressed into pellets, and sealed in an evacuated quartz ampoule, which was heated at 1000 °C for 48 hours.

Structural characterization. High-resolution powder X-ray diffraction data were collected at beamline ID22 at the European Synchrotron Radiation Facility, using a multianalyser stage detector and 27.5 keV radiation (λ = 0.450842 Å). Data were collected on warming, with the sample loaded in a 0.5 mm diameter borosilicate capillary and heated from room temperature to 500 K using a nitrogen cryostream. X-ray total scattering data were also collected at ID22. In order to access the high momentum transfers Q needed to generate good quality PDFs, a Perkin Elmer XRD1611 2D detector and 60 keV radiation (λ = 0.206547 Å) were used. The sample was held in a 0.7 mm diameter quartz capillary and heated from 300 to 1100 K using a hot air blower, with measurements made on warming. 201 exposures were collected at each temperature step and averaged to give a total scattering pattern. Rietveld analysis was performed using GSAS.[24] Total scattering functions $S(Q)$ were transformed to PDFs $G(r)$ using PDFgetX3,[25] for $0.5 \leq Q$ (Å^{-1}) ≤ 25.8, after making suitable background corrections. Structural models were refined against $G(r)$ using PDFgui,[26] which includes simulation of termination ripples, for interatomic distances $1.5 \leq r$ (Å) ≤ 12.

Powder neutron diffraction was carried out with the HRPD beamline at the ISIS pulsed neutron and muon source. A 2.7 g sample in a vanadium can was loaded into a furnace, heated to 550 K, and data were collected on cooling to room temperature. Diffraction patterns collected by the 168° detectors were analysed by Rietveld refinement using GSAS.

Magnetic and transport property measurements. The magnetic behaviour of GaV_2O_4 was measured using a Quantum Design SQUID MPMS XL. Measurements were made over the temperature range 2-300 K in an applied field of 100 Oe, under zero-field cooled and field cooled conditions, and on heating from 300 to 600 K in an applied field of 5000 Oe. The electrical resistivity of a sintered pellet of GaV_2O_4 was measured over the range 300-800 K by a conventional four-probe technique, using in-house apparatus.

Quasi-elastic neutron scattering. QENS data were collected with the time-of-flight spectrometer IN6 at the Institut Laue Langevin. The sample was loaded into a niobium can in a furnace, and spectra were collected between 400 K and 1100 K using neutrons with incident wavelength λ = 5.12 Å. Eight spectra were collected at each temperature and averaged scattering functions $S(Q,E)$, where E is the energy transfer, were generated with vanadium normalization and corrections for the empty can background.

RESULTS AND DISCUSSION

Average structure. High-resolution powder X-ray diffraction was used to study the average structure of GaV_2O_4, and a distortion analogous to that found in AlV_2O_4[20] is observed. At room temperature, GaV_2O_4 has an $R\bar{3}m$ unit cell (Figure 1): Rietveld analysis (Figure 2a) gives lattice parameters a_H = 5.86207(4) Å and c_H = 28.98269(37) Å, and the refined atomic parameters are given in Table 1. Bond distances and angles are provided in the Supporting Information. There are three vanadium crystallographic sites, and refinement of their positions defines V_3 trimers and V_4 tetramers through short (~2.80 Å) V-V nearest-neighbor distances. Tetramers are formed by the V2 site and half of the V3 site cations; the remaining V3 cations form trimers, and the V1 site is non-bonding (Figure 1a). In this low temperature phase, pairs of a V_3 cluster and V_4 cluster have long-range structural order but there are two possible configurations of the clusters within each pair. This disorder in the average structure is modelled by splitting the V2 site (Figure 1b). An impurity phase, V_2O_3, with weight fraction 5.3% was also found in the Rietveld fits.

On heating, a structural phase transition from the $R\bar{3}m$ superstructure to the cubic $Fd\bar{3}m$ normal spinel arrangement is observed. Within this average structure there is only a single $V^{2.5+}$ crystallographic site and all V-V nearest-neighbor distances are equivalent (~2.95 Å). However, as found for AlV_2O_4, Rietveld fits are improved by letting 7/8 of the vanadium (the proportion of vanadium cations involved in orbital molecule bonding) displace away from this ideal position as a split site, indicating disorder in the high temperature phase.

Table 1. Atomic parameters of $R\bar{3}m$ GaV_2O_4 at room temperature, from Rietveld refinement against the high-resolution powder X-ray diffraction data.

Atom	*Site*	*x*	*y*	*z*	*Occupancy*	U_{iso} (Å²)
Ga1	*6c*	*0*	*0*	*0.18489(9)*	*1*	*0.0069(1)*
Ga2	*6c*	*0*	*0*	*0.31051(9)*	*1*	
V1	*3a*	*0*	*0*	*0*	*1*	*0.0059(2)*
V2	*6c*	*0*	*0*	*0.49537(32)*	*0.5*	
V3	*18h*	*0.83982(19)*	*0.16018(19)*	*0.41668(9)*	*1*	
O1	*6c*	*0*	*0*	*0.12468(44)*	*1*	*0.0103(4)*
O2	*6c*	*0*	*0*	*0.37486(40)*	*1*	
O3	*18h*	*0.83614(70)*	*0.16386(70)*	*0.54152(29)*	*1*	
O4	*18h*	*0.82758(70)*	*0.17242(70)*	*0.28884(28)*	*1*	

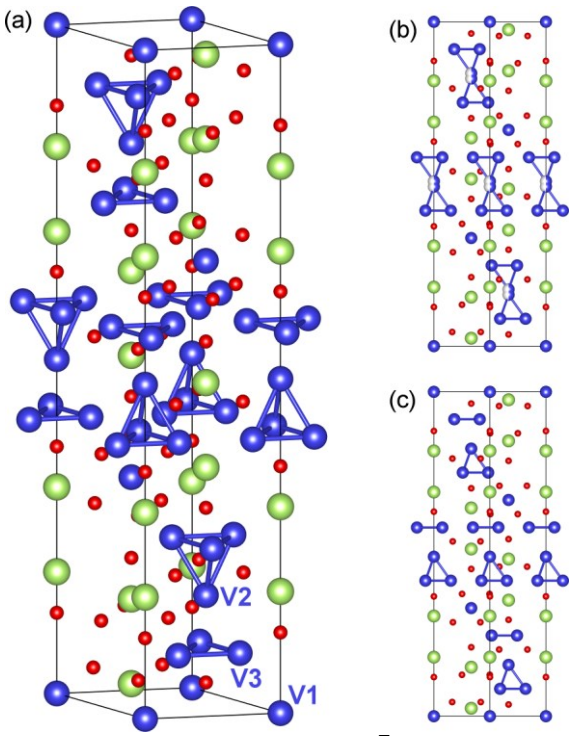

Figure 1. (a) Local structure in the $R\bar{3}m$ phase of GaV_2O_4. Ga (green), V (blue) and O (red) are shown, with the three different vanadium sites labeled and the short (~2.80 Å) V-V separations defining the V_3 trimers and V_4 tetramers shown. One local configuration of each orbital molecule pair is shown here but these are disordered over two possible configurations (trimer-tetramer or tetramer-trimer) in the average structure, shown in (b), which is modelled by splitting the *z*-coordinate of the V2 site in Rietveld refinements. (c) The *R*3*m* structure used for PDF fits, in which all orbital molecule pairs have the same orientation.

Conversion of the high temperature $Fd\bar{3}m$ structure into the low temperature $R\bar{3}m$ structure is evident as a splitting of the Bragg peaks of the cubic phase (Figure 2a, insets), as the rhombohedral distortion causes the lattice parameters a_H and c_H to deviate from metrically cubic values $a_H = a_C/\sqrt{2}$ and $c_H = \sqrt{12}a_C$. The thermal variation of an order parameter-like quantity X below the long-range ordering transition temperature T_{CO} can be described by the critical equation:

$$X = X_{CO} + (X_0 - X_{CO})\tanh\left(W_X t^{1/2}\right) / \tanh(W_X) \quad (1)$$

where X takes values X_0 and X_{CO} at T = 0 and $T = T_{CO}$, respectively; the reduced temperature is $t = (T_{CO} - T)/T_{CO}$; and $W_X \approx 2$ is a fitting parameter. Equation 1 has been used to describe the behavior of structural quantities below the Verwey transition in magnetite.[27] Applying Eq 1 to the thermal variation of the reduced lattice parameters of GaV_2O_4, $\sqrt{2}a_H$ and $c_H/\sqrt{12}$, taken from Rietveld refinements, gives good fits and determines T_{CO} = 415 K (Figure 3a).

Powder neutron diffraction (Figure 2b) corroborates the above structural characterization, although as a result of poor thermal equilibration of the large sample used for this experiment the value of T_{CO} appears as 465 K. As vanadium scatters neutrons very weakly no site splitting to describe disordered orbital molecules was included in the refinement models. However, the high neutron scattering contrast between Ga and V confirms that there is no antisite disorder.

Both the X-ray and neutron refinements reveal that a proportion of GaV_2O_4 remains cubic below T_{CO}. This is most likely due to microstructural stresses that prevent some regions of the polycrystalline sample from converting to rhombohedral below the transition. A similar suppression of the orbital molecule ordering transition in strained crystallites has been observed in magnetite.[27] The fractions of the two GaV_2O_4 phases were extracted through Rietveld refinement, and the decreasing fraction of the $R\bar{3}m$ phase on warming is described well by Eq 1 (Figure 3b).

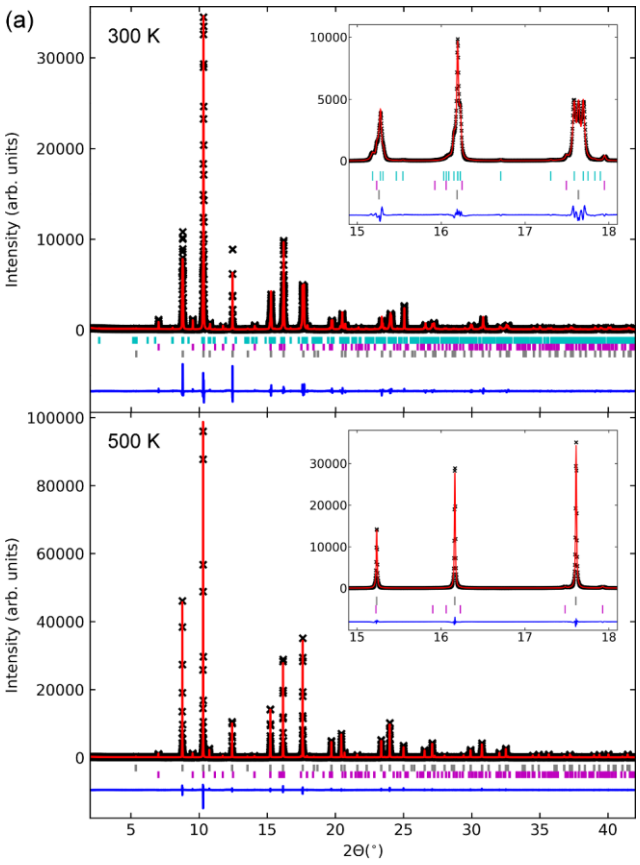

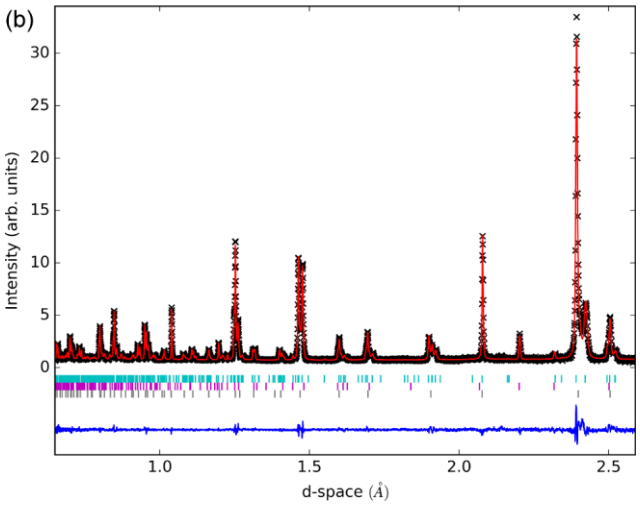

Figure 2. Rietveld analyses of GaV_2O_4. Tick marks correspond to the $R\bar{3}m$ (blue) and $Fd\bar{3}m$ (grey) phases of GaV_2O_4, and a V_2O_3 impurity (pink). (a) Fits to high-resolution powder X-ray diffraction data collected at room temperature (upper, R_w = 12.3%) and 500 K (lower, R_w = 9.0%), with insets showing the peak splitting associated with the rhombohedral distortion in an expanded region. (b) Fit to powder neutron diffraction data collected at room temperature (R_w = 5.7%).

Rietveld fits to neutron diffraction data collected in the critical region were used to determine the lattice parameters of the rhombohedral (a_H and c_H) and cubic (a_C) phases, and the spontaneous strains for the low temperature phase were calculated as:

$$s_a = \frac{\sqrt{2}a_H - a_C}{a_C} \quad (2)$$

$$s_c = \frac{c_H/\sqrt{12} - a_C}{a_C} \quad (3)$$

Spontaneous strain is an order parameter and for a (near) second-order transition close to the transition temperature the variation:

$$s^2 = s_0^2\left(1 - \frac{T}{T_{CO}}\right) \quad (4)$$

is expected. Plots of s_a^2 and s_c^2 against T/T_{CO} confirm the quasi-continuous nature of the structural transition (Figure 3c).

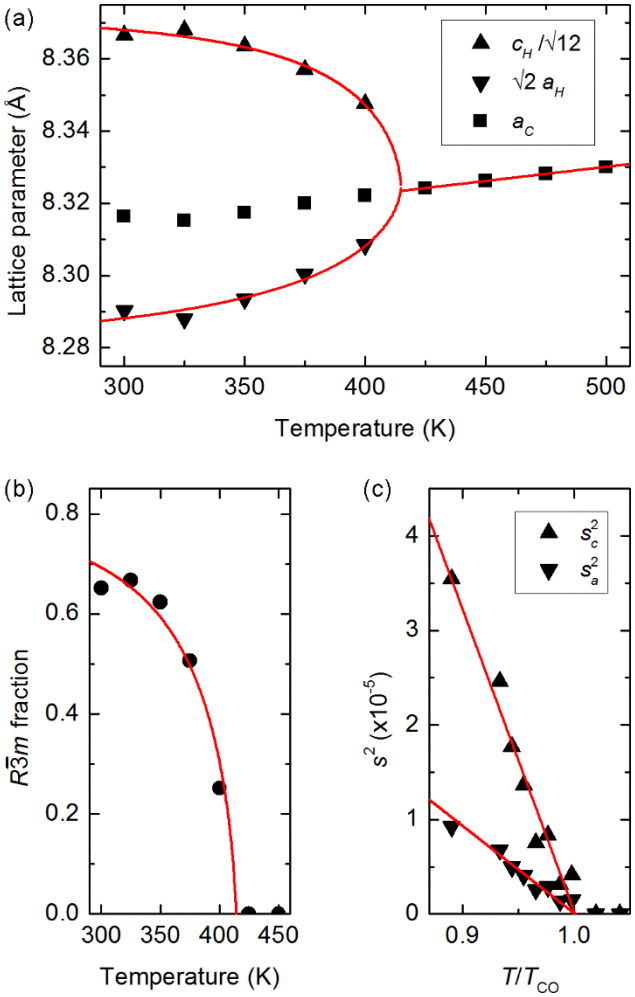

Figure 3. (a) Lattice parameters of the rhombohedral and cubic phases of GaV_2O_4, and (b) the rhombohedral phase fraction, from high-resolution powder X-ray diffraction showing fits of Eq 1 below T_{CO} = 415 K. (c) Squared spontaneous lattice strains of rhombohedral GaV_2O_4 from powder neutron diffraction fits decrease linearly to zero at $T = T_{CO}$, in keeping with Eq 4 for a continuous transition.

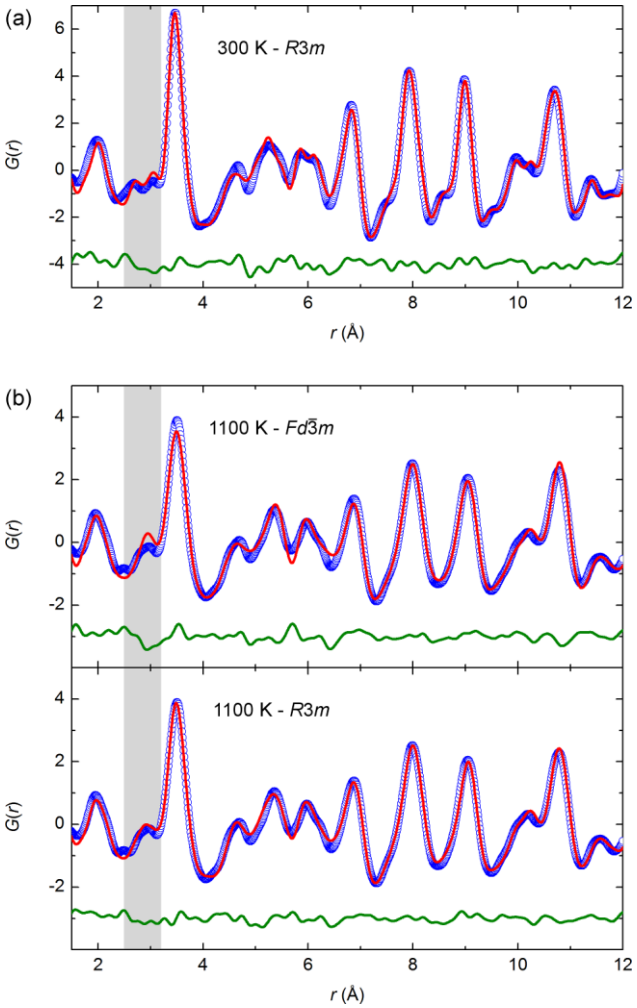

Figure 4. (a) Fit of the *R*3*m* model, featuring V_3 and V_4 orbital molecules, to the 300 K PDF of GaV_2O_4 (R_w = 11.9%) where the presence of short and long V-V distances gives rise to two peaks in the shaded region. (b) Fits to the 1100 K PDF using the *Fd*$\bar{3}$*m* average structure model (upper, R_w = 13.5%), in which all V-V nearest-neighbor distances are equal, and the *R*3*m* model representing disordered orbital molecules (lower, R_w = 10.3%).

Local structure. X-ray total scattering data have been used to characterize the local V-V interactions in GaV_2O_4. Rietveld analyses of these data, using the split-site *R*$\bar{3}$*m* and *Fd*$\bar{3}$*m* models described previously, are consistent with those using the high-resolution powder diffraction data. Analysis of the PDFs generated from the total scattering data shows that the real-space structure described by the PDFs is consistent with that determined from Rietveld refinement below T_{CO}, with ordered pairs of V_3 and V_4 orbital molecules (Figure 4a). A modified model was used to fit these PDFs – instead of *R*$\bar{3}$*m* symmetry with a split V2 site a lower symmetry *R*3*m* model, in which the V2 site displaces with full occupancy, was used (though constraints consistent with *R*$\bar{3}$*m* symmetry were applied to all other sites to reduce the number of refined variables).

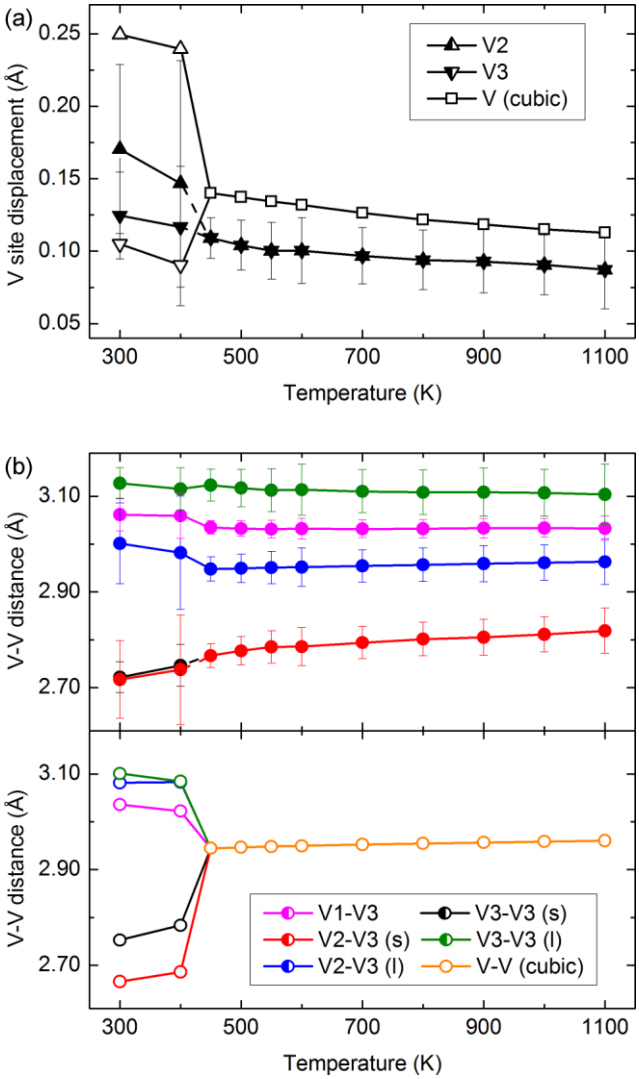

Figure 5. Structural parameters extracted from PDF (filled symbols) and Rietveld (open symbols) analyses of the X-ray total scattering data, evidencing the persistence of disordered orbital molecules to 1100 K. (a) V-V bonding causes the vanadium atoms to be displaced from ideal spinel positions. The V2 and V3 sites displace independently below T_{CO}, with the split-site *R*$\bar{3}$*m* model used for Rietveld fits and the *R*3*m* model for PDF fits. Above T_{CO} Rietveld analysis using the split-site *Fd*$\bar{3}$*m* model reveals significant displacement of vanadium away from its ideal site, and PDF fits using the *R*3*m* model yield similar displacements (for refinement stability, the V2 and V3 site displacements were constrained to be equal). (b) PDF fits reveal that the short V-V distances that define the ordered V_3 and V_4 orbital molecules in the ground state evolve continuously through T_{CO}, though Rietveld analysis of the cubic average structure gives only a single V-V distance.

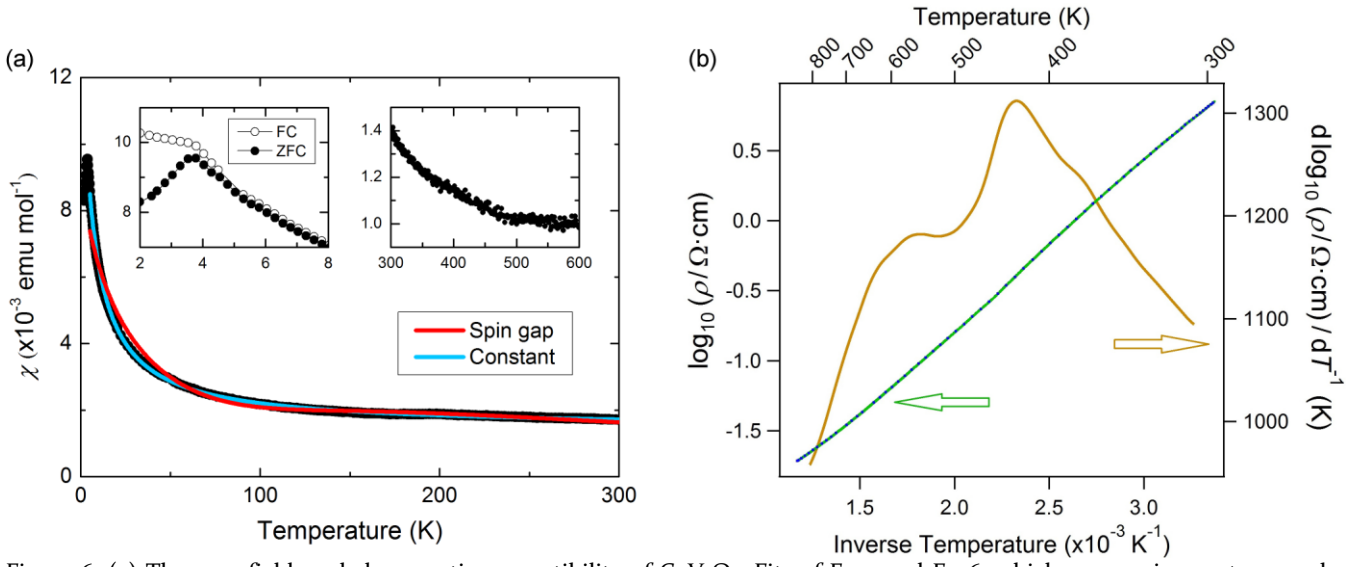

Figure 6. (a) The zero-field cooled magnetic susceptibility of GaV_2O_4. Fits of Eq 5 and Eq 6, which use a spin-gap term and a constant, respectively, to account for the susceptibility contributions of the spin-singlet clusters, are shown over the range 5-300 K. Left inset: a cusp, resulting from freezing or ordering of paramagnetic V^{3+} spins not involved in orbital molecule bonding, at 3.8 K. Right inset: the high temperature susceptibility measured on warming, with no pronounced anomaly at T_{CO} = 415 K. (b) Logarithmic plot of high temperature resistivity against inverse temperature showing continuous variation through T_{CO}, but with a change of slope at T_{CO} = 415 K evident in the derivative.

Both the $R\bar{3}m$ and $R3m$ models feature V_3-V_4 orbital molecule pairs, so the local structural correlations in both are the same. However, whilst in the $R\bar{3}m$ model different pairs adopt different configurations and are disordered, in the $R3m$ model all pairs have the same orientation. The two models therefore represent different average structures (Figures 1b and 1c). As the $R\bar{3}m$ model gives a better Rietveld fit than the $R3m$ model, the disordered pairs scenario is a better overall description of the structure of rhombohedral GaV_2O_4, as was also found for AlV_2O_4.[20] The $R3m$ model was used for the PDF fits as the half-occupied split-site used to model the disorder in the $R\bar{3}m$ model, whilst suitable for describing the average atomic distribution, does not meaningfully represent the local structure.

Above 415 K, the PDFs are not well fit by an ideal cubic spinel model in which the V-V nearest-neighbor distances are equal (Figure 4b). This is particularly evident in the first V-V coordination shell, which corresponds to the PDF intensity in the range $2.5 \leq r$ (Å) ≤ 3.2 (the shaded region in Figure 4), indicative of local V site displacements. A much better fit is achieved using the same $R3m$ model as used to fit the PDFs below T_{CO}. a_H and c_H were constrained in the metrically cubic ratio, consistent with the average structure, and the V2 and V3 site displacements were constrained to be equal to improve refinement stability (consequently, the two short bonding V-V distances are equal). V site displacements of ~0.1 Å, consistent with those found through split-site Rietveld refinements, are present to 1100 K (Figure 5a), and result in short V-V distances corresponding to locally ordered V_3 and V_4 orbital molecules (Figure 5b). The V-V distances determined at 300 K and 1100 K are tabulated in the Supporting Information. The residual cubic phase below T_{CO} was not included in the analysis of the X-ray total scattering data: the resolution of the diffraction patterns is insufficient for it to be included in Rietveld fits, and as both phases of GaV_2O_4 are likely to have the same local structure it does not need to be accounted for separately in the PDF analysis.

The persistence of the orbital molecules to high temperatures in GaV_2O_4, with T_{CO} indicating their order-disorder transition, is consistent with the orbital molecule behavior found in AlV_2O_4,[20] though the value of T_{CO} = 415 K in GaV_2O_4 is substantially lower than that for AlV_2O_4 (700 K). This is likely due to Ga^{3+} having a larger ionic radius than Al^{3+}, so the average lattice V-V separation – 2.96 Å in GaV_2O_4 at 1100 K, compared to 2.92 Å in AlV_2O_4 – is correspondingly larger. This weakens the tendency of orbital molecules to long-range order and hence suppresses T_{CO}. Furthermore, the larger average separation weakens the interactions within the orbital molecules. Not only are the bonding V-V distances in GaV_2O_4 (both 2.72 Å at 300 K) not as short as those in AlV_2O_4 (2.59 Å and 2.65 Å), but the difference between bonding and non-bonding distances (2.72-3.13 Å in GaV_2O_4, 2.59-3.17 Å in AlV_2O_4) is less. The smaller spin-gap energy, discussed in the following section, also evidences weaker bonding interactions in GaV_2O_4.

A lower T_{CO} does, however, allow the temperature scale over which local orbital molecule interactions are found to be extended. The total scattering analysis demonstrates the persistence of structurally disordered orbital molecules in GaV_2O_4 to 1100 K which is $2.7T_{CO}$, far above the critical regime.

Magnetic and transport properties. Although the presence of orbital molecules in GaV_2O_4 has been deduced through structural analysis and the identification of unusually short V-V distances, their presence impacts on, and can be corroborated by characterizing, the material's magnetic and electrical properties. The formation of orbital molecules requires electrons to be paired in V-V bonds, and the properties of GaV_2O_4 are based on the electronic description $Ga_4[V_4^{8+}V_3^{9+}V^{3+}]O_{16}$. For every eight vanadium atoms, which have an average oxidation state of 2.5, a V_4^{8+} tetramer and a V_3^{9+} trimer are formed by the two-center two-electron bonding of four V^{2+} and three V^{3+}, respectively. These are both spin-paired (S = 0) species, but the remaining vanadium is a monomeric and paramagnetic (S = 1) V^{3+} cation.

Equation 5, used previously to characterize the magnetic behavior of AlV_2O_4,[21] treats the total susceptibility as the sum of a Curie-Weiss term for the monomeric V^{3+} cations, and a generic spin-gap term for the spin-singlet clusters, which can be thermally excited to a triplet state:

$$\chi = \frac{C}{T-\theta} + \frac{D}{T[1+\frac{1}{3}\exp\left(\frac{E_g}{k_B T}\right)]} \quad (5)$$

Equation 5 gives a reasonable fit to the measured susceptibility of GaV_2O_4, with parameters C = 0.225 emu K mol^{-1}, θ = -25.4 K, D = 0.662 emu K mol^{-1}, and E_g/k_B = 416.2 K (Figure 6a). These values are in keeping with those determined for AlV_2O_4, and give a paramagnetic moment μ_{eff} = 2.68 μ_B (the predicted values for a d^2 cation are C = 0.25 emu K mol^{-1} and μ_{eff} = 2.83 μ_B). The average spin-gap energy E_g/k_B = 416 K shows that strong spin pairing is present, though a smaller value than for AlV_2O_4 (844 K) is consistent with GaV_2O_4 having weaker bonding interactions. An improved fit to the low temperature susceptibility is, however, obtained by using a temperature-independent constant to account for the susceptibility contributions of the orbital molecules:

$$\chi = \frac{C}{T-\theta} + A \quad (6)$$

with fitting parameters C = 0.0793 emu K mol^{-1}, θ = -6.2 K and A = 1.46 x10^{-3} emu mol^{-1}. A negative value of θ, indicating antiferromagnetic correlations of the V^{3+} spins, is again obtained, though the value of C gives a moment μ_{eff} = 1.59 μ_B that is smaller than expected for S = 1 V^{3+}. A sharp cusp in the susceptibility, below which the zero-field cooled and field cooled susceptibilities diverge, is observed at 3.8 K and is attributed to the freezing or ordering of the monomeric V^{3+} spins.

Although a structural distortion occurs in GaV_2O_4 at T_{CO} = 415 K, no corresponding change in the high temperature susceptibility is observed. This is consistent with the structural description of local V_3 and V_4 orbital molecules persisting above T_{CO}, as the breakup of these spin-singlet clusters should lead to large increases of the susceptibility – complete decomposition would lead to C = 2.88 emu K mol^{-1} for paramagnetic $GaV^{2+}V^{3+}O_4$. Similarly, there is no change in resistivity that might arise if the bonding electrons became delocalized (Figure 6b). GaV_2O_4 is a semiconductor with an activation energy of 0.24 eV, and only a slight change of slope is observed around T_{CO}. Equivalent measurements of the properties of AlV_2O_4 also only show small changes to the susceptibility and resistivity on crossing T_{CO}.[22] Hence the physical properties of these materials are consistent with a change from ordered to disordered orbital molecules at the transition, rather than any changes in the V-V bonding.

Quasi-elastic neutron scattering. The total scattering analysis and property measurements described previously demonstrate the persistence of structurally disordered orbital molecules in GaV_2O_4 (as in AlV_2O_4) to 1100 K. However, from these analyses it is not clear whether the disordered orbital molecules in these materials are static (glass-like) or dynamic (liquid-like). QENS has been used to investigate whether dynamical motion or interchange of V atoms between orbital molecules in GaV_2O_4 becomes evident at high temperatures. Dynamic behavior would result in quasi-elastic scattering, which would appear as a broadening of the elastic scattering line.

QENS data were collected from 400 K, at which temperature the orbital molecule pairs have long-range order and are expected to be static, to 1100 K. The scattering functions $S(Q,E)$ at 400 K and 1100 K are provided in the Supporting Information, and the integrated functions $S(E)$ for all measured temperatures are plotted in Figure 7. Although the intensity of the elastic line decreases on heating, due to the Debye-Waller effect, no broadening of the elastic line is observed. This linewidth establishes that in GaV_2O_4 any dynamic behaviour must be slower than ~10^{-11}s, indicating that the clusters are well defined and statically disordered even at 1100 K.

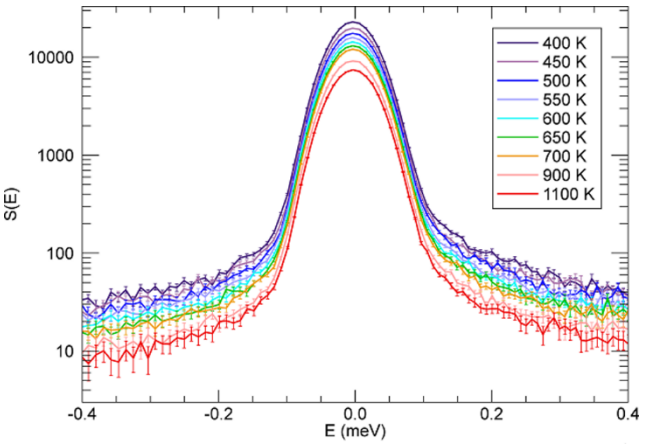

Figure 7. Thermal variation of the QENS scattering function $S(Q,E)$ for GaV_2O_4, integrated over the full measured range of Q. Quasi-elastic scattering from orbital molecule dynamics that would broaden the elastic line is not seen, showing that the disordered orbital molecules remain static up to 1100 K.

CONCLUSION

GaV_2O_4, a new oxide spinel, has been synthesized. Long-range orbital- and charge-ordering in the ground state results in a structural distortion and pairwise order of V_3^{9+} and V_4^{8+} orbital molecules. Above T_{CO} = 415 K, long-range order is lost but short-range order remains, and the orbital molecules persist in a statically disordered phase to at least $2.7T_{CO}$.

The orbital molecules in GaV_2O_4 and AlV_2O_4 are found to be stable to temperatures well above that at which they lose long-range structural order, unlike those in VO_2 which do not persist above the metal-insulator transition. This implies that the electronic interactions that result in V-V bonding in vanadium oxides can vary considerably, from real-space (molecular) to momentum-space (Fermi surface) electronic instabilities. To explore these variations of orbital molecule bonding, further investigations of the local and long-range structures of vanadium oxides will be required.

ASSOCIATED CONTENT

Supporting Information. Metal-oxygen bond distances and angles in the room temperature structure; V-V distances at 300 K and 1100 K; and QENS scattering functions at 400 K and 1100 K. This material is available free of charge via the Internet at http://pubs.acs.org.

AUTHOR INFORMATION

Corresponding Author

*E-mail: j.p.attfield@ed.ac.uk

Author Contributions

A.J.B., S.A.J.K. and J.P.A. designed the concept for this study. A.J.B. performed the experimental work and data analysis and C.L. made the resistivity measurement. A.J.B. and J.P.A. wrote the manuscript with inputs from all authors.

Funding Sources

This work was supported by the ERC (Advanced Grant EC339312) and access to facilities was provided by the STFC. This manuscript has been authored by UT-Battelle, LLC under Contract No. DE-AC05-00OR22725 with the U.S. Department of Energy. The United States Government retains and the publisher, by accepting the article for publication, acknowledges that the United States Government retains a non-exclusive, paid-up, irrevocable, worldwide license to publish or reproduce the published form of this manuscript, or allow others to do so, for United States Government purposes. The Department of Energy will provide public access to these results of federally sponsored research in accordance with the DOE Public Access Plan (http://energy.gov/downloads/doe-public-access-plan).

Notes

The authors declare no competing financial interest.

ACKNOWLEDGMENT

We thank Mauro Coduri (ESRF), Kevin Knight (ISIS) and Michael Koza (ILL) for help with data collection; Ka H. Hong for assistance at ESRF; and James Cumby and Paul M. Sarte for assistance with data analysis.

ABBREVIATIONS

PDF, pair distribution function; QENS, quasi-elastic neutron scattering.

REFERENCES

(1) Armstrong, A.R.; Lyness, C.; Panchmatia, P. M.; Islam, M. S.; Bruce, P. G. The lithium intercalation process in the low-voltage lithium battery anode $Li_{1+x}V_{1-x}O_2$. *Nat. Mater.* **2011**, *10*, 223-229.

(2) Guignard, M.; Didier, C.; Darriet, J.; Bordet, P.; Elkaïm, E.; Delmas, C. P2-Na_xVO_2 system as electrodes for batteries and electron-correlated materials. *Nat. Mater.* **2013**, *12*, 74-80.

(3) Wang, Y.; Cao, G. Developments in Nanostructured Cathode Materials for High-Performance Lithium-Ion Batteries. *Adv. Mater.* **2008**, *20*, 2251-2269.

(4) Butt, F. K.; Tahir, M.; Cao, C.; Idrees, F.; Ahmed, R.; Khan, W. S.; Ali, Z.; Mahmood, N.; Tanveer, M.; Mahmood, A.; Aslam, I. Synthesis of Novel ZnV_2O_4 Hierarchical Nanospheres and Their Applications as Electrochemical Supercapacitor and Hydrogen Storage Material. *Appl. Mater. Interfaces.* **2014**, *6*, 13635-13641.

(5) Sammes, N. M.; Tompsett, G. A.; Näfe, H.; Aldinger, F. Bismuth Based Oxide Electrolytes – Structure and Ionic Conductivity. *J. Eur. Ceram. Soc.* **1999**, *19*, 1801-1826.

(6) Wachs, I. E. Catalysis science of supported vanadium oxide catalysts. *Dalton Trans.* **2013**, *42*, 11762-11769.

(7) Morin, F. J. Oxides which show a metal-to-insulator transition at the Neel temperature. *Phys. Rev. Lett.* **1959**, *3*, 34-36.

(8) Yang, Z.; Ko, C.; Ramanathan, S. Oxide Electronics Utilizing Ultrafast Metal-Insulator Transitions. *Annu. Rev. Mater. Res.* **2011**, *41*, 337-367.

(9) Wang, S.; Liu, M.; Kong, L.; Long, Y.; Jiang, X.; Yu, A. Recent progress in VO_2 smart coatings: Strategies to improve the thermochromic properties. *Prog. Mater. Sci.* **2016**, *81*, 1-54.

(10) Goodenough, J. B. The Two Components of the Crystallographic Transition in VO_2. *J. Solid State Chem.* **1971**, *3*, 490-500.

(11) Attfield, J. P. Orbital molecules in electronic materials. *APL Mater.* **2015**, *3*, 041510.

(12) Marezio, M.; McWhan, D. B.; Dernier, P. D.; Remeika, J. P. Structural Aspects of the Metal-Insulator Transition in V_4O_7. *J. Solid State Chem.* **1973**, *6*, 419-429.

(13) Pourpoint, F.; Hua, X.; Middlemiss, D. S.; Adamson, P.; Wang, D.; Bruce, P. G.; Grey, C. P. New Insights into the Crystal and Electronic Structures of $Li_{1+x}V_{1-x}O_2$ from Solid State NMR, Pair Distribution Function Analyses, and First Principles Calculations. *Chem. Mater.* **2012**, *24*, 2880-2893.

(14) Kajita, T.; Kanzaki, T.; Suzuki, T.; Kim, J. E.; Kato, K.; Takata, M.; Katsufuji, T. Opening of a charge gap with V trimerization in $BaV_{10}O_{15}$. *Phys. Rev. B.* **2010**, *81*, 060405(R).

(15) McQueen, T. M.; Stephens, P. W.; Huang, Q.; Klimczuk, T.; Ronning, F.; Cava, R. J. Successive Orbital Ordering Transitions in $NaVO_2$. *Phys. Rev. Lett.* **2008**, *101*, 166402.

(16) Guignard, M.; Delmas, C. Using a Battery to Synthesize New Vanadium Oxides. *ChemistrySelect* **2017**, *2*, 5800-5804.

(17) Haverkort, M. W.; Hu, Z.; Tanaka, A.; Reichelt, W.; Streltsov, S. V.; Korotin, M. A.; Anisimov, V. I.; Hsieh, H. H.; Lin, H. J.; Chen, C. T.; Khomskii, D. I.; Tjeng, L. H. Orbital-assisted metal-insulator transition in VO_2. *Phys. Rev. Lett.* **2005**, *95*, 196404.

(18) Jin-no, T.; Shimizu, Y.; Itoh, M.; Niitaka, S.; Takagi, H. Orbital reformation with vanadium trimerization in d^2 triangular lattice $LiVO_2$ revealed by ^{51}V NMR. *Phys. Rev. B.* **2013**, *87*, 075135.

(19) Khomskii, D. I.; Mizokawa, T. Orbitally Induced Peierls State in Spinels. *Phys. Rev. Lett.* **2005**, *94*, 156402.

(20) Browne, A. J.; Kimber, S. A. J.; Attfield, J. P. Persistent three- and four-atom orbital molecules in the spinel AlV_2O_4. *Phys. Rev. Mater.* **2017**, *1*, 052003(R).

(21) Horibe, Y; Shingu, M.; Kurushima, K.; Ishibashi, H.; Ikeda, N.; Kato, K.; Motome, Y.; Furukawa, N.; Mori, S.; Katsufuji, T. Spontaneous Formation of Vanadium "Molecules" in a Geometrically Frustrated Crystal: AlV_2O_4. *Phys. Rev. Lett.* **2006**, *96*, 086406.

(22) Matsuno, K.; Katsufuji, T.; Mori, S.; Moritomo, Y.; Machida, A.; Nishibori, E.; Takata, M.; Sakata, M.; Yamamoto, N.; Takagi, H. Charge Ordering in the Geometrically Frustrated Spinel AlV_2O_4. *J. Phys. Soc. Jpn.* **2001**, *70*, 1456-1459.

(23) Corr, S. A.; Shoemaker, D. P.; Melot, B. C.; Seshadri, R. Real-Space Investigation of Structural Changes at the Metal-Insulator Transition in VO_2. *Phys. Rev. Lett.* **2010**, *105*, 056404.

(24) Larson, A. C.; Von Dreele, R. B. *General Structure Analysis System (GSAS)*; Los Alamos National Laboratory Report LAUR 86-748, 2004.

(25) Juhás, P.; Davis, T.; Farrow, C. L.; Billinge, S. J. L. PDFgetX3: A rapid and highly automatable program for processing powder diffraction data into total scattering pair distribution functions. *J. Appl. Crystallogr.* **2013**, *46*, 560-566.

(26) Farrow, C. L.; Juhas, P.; Liu, J. W.; Bryndin, D.; Božin, E. S.; Bloch, J.; Proffen, Th.; Billinge, S. J. L. PDFfit2 and PDFgui: computer programs for studying nanostructure in crystals. *J. Phys.: Condens. Matter.* **2007**, *19*, 335219.

(27) Senn, M. S.; Wright, J. P.; Cumby, J.; Attfield, J. P. Charge localization in the Verwey structure of magnetite. *Phys. Rev. B.* **2015**, *92*, 024104.

For table of contents only:

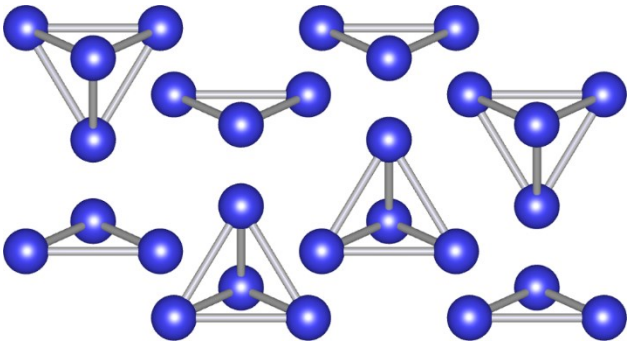

Synopsis:

GaV_2O_4, a new vanadium spinel, has been synthesized. Powder diffraction and X-ray total scattering studies, complemented by magnetization and resistivity measurements, reveal that the low temperature phase of this material is structurally distorted and features ordered three- and four-atom vanadium clusters. These clusters persist into a disordered cubic phase above T_{CO} = 415 K. Furthermore, quasi-elastic neutron scattering indicates that the disordered clusters remain well defined and static to 1100 K.